Published in final edited form as:

Invest Radiol. 2016 September ; 51(9): 575–581. doi:10.1097/RLI.0000000000000269.

MR Elastography of the liver: qualitative and quantitative comparison of gradient echo and spin echo echoplanar imaging sequences

Mathilde Wagner, MD, PhD[1], **Cecilia Besa, MD**[1,2], **Jad Bou Ayache, MD**[1,2], **Temel Kaya Yasar, PhD**[1], **Octavia Bane, PhD**[1], **Maggie Fung, MEng**[4], **Richard L. Ehman, MD**[3], and **Bachir Taouli, MD**[1,2]

[1]Translational and Molecular Imaging Institute, Icahn School of Medicine at Mount Sinai, New York, NY, United States

[2]Department of Radiology, Icahn School of Medicine at Mount Sinai, New York, NY, United States

[3]Department of Radiology, Mayo Clinic, Rochester, Minnesota, United States

[4]GE Healthcare, MR Applications & Workflow, New York, NY, United States

Abstract

Objective—To compare 2D gradient recalled echo (GRE) and 2D spin echo echoplanar imaging (SE-EPI) magnetic resonance elastography (MRE) sequences of the liver in terms of image quality and quantitative liver stiffness (LS) measurement.

Materials and methods—This prospective study involved 50 consecutive subjects (M/F 33/17, mean age 58 y) who underwent liver MRI at 3.0T including two MRE sequences, 2D GRE and 2D SE-EPI (acquisition time 56 vs 16 s, respectively). Image quality scores were assessed by two independent observers based on wave propagation and organ coverage on the confidence map (range 0–15). A third observer measured LS on stiffness maps (in kPa). Mean LS values, ROI size (based on confidence map) and image quality scores between SE-EPI and GRE-MRE were compared using paired nonparametric Wilcoxon test. Reproducibility of LS values between the two sequences was assessed using intraclass coefficient correlation (ICC), coefficient of variation (CV) and Bland-Altman limits of agreement (BALA). T2* effect on image quality was assessed using partial Spearman correlation.

Results—There were 4 cases of failure with GRE-MRE and none with SE-EPI-MRE. Image quality scores and ROI size were significantly higher using SE-EPI-MRE vs. GRE-MRE ($p < 0.0001$ for both measurements and observers). LS measurements were not significantly different between the two sequences (3.75 ± 1.87 vs. 3.51 ± 1.53 kPa, $p=0.062$), were significantly correlated (ICC=0.909) and had excellent reproducibility (CV=10.2%, bias=0.023, BALA −1.19; 1.66 kPa). Image quality scores using GRE-MRE were significantly correlated with T2*, while there was no correlation for SE-EPI-MRE.

Corresponding author: Bachir Taouli, MD, Icahn School of Medicine at Mount Sinai, Department of Radiology and Translational and Molecular Imaging Institute, 1470 Madison Avenue, Room 107, New York, NY 10029 USA, bachir.taouli@mountsinai.org, Tel: 212 824 8453, Fax: 646 537 9589.

Conclusion—Our data suggest that suggest that SE-EPI-MRE may be a better alternative to GRE-MRE. The diagnostic performance of SE-EPI-MRE for detection of liver fibrosis needs to be assessed in a future study.

Keywords

Liver stiffness; MR elastography; Gradient Recalled Echo; Spin Echo Echoplanar

INTRODUCTION

Magnetic Resonance Elastography (MRE) is a non-invasive imaging method that estimates mechanical properties of tissues. MRE is based on a phase contrast imaging method which images mechanical wave propagation, and assesses tissue stiffness. Using MRE, it is possible to quantify liver stiffness (LS), which can be used to non-invasively detect liver fibrosis and cirrhosis (1). Liver stiffness measurement can also be used to detect and assess severity of portal hypertension (2, 3), in addition to spleen stiffness (4). Multiple studies showed high accuracy of MRE for liver fibrosis detection and stratification with equivalent to higher performance than other noninvasive modalities, including transient elastography and serum markers (5–8). Moreover, MRE provides larger sampling compared to ultrasound (US) elastography techniques with high repeatability of LS measurements (9, 10).

MRE needs the addition of motion encoding gradients (MEGs) in order to image the wave propagation and to compute tissue stiffness. The most common pulse sequence used for liver MRE is based on Gradient Recalled Echo (GRE) (11). In this sequence, the MEGs are usually applied along the z-axis, with the same frequency as the mechanical excitation and are synchronized with it. This allows the advantage to give precise motion encoding. The addition of the MEGs increases the echo time (TE) (12), which may decrease signal-to-noise ratio (SNR) on GRE images and cause MRE failure in patients with hepatic iron overload where the T2* decay time of the liver tissue is short (7, 13). This limitation may be overcome by using a Spin Echo (SE) based Echo Planar Imaging (EPI) MRE pulse sequence with shorter TE. Fractional encoding is applied in SE-EPI pulse sequences in order to achieve short enough TE (14, 15). As SE-EPI-MRE pulse sequences are less affected by T2* decay, this method may decrease the risk of failure in case of iron overload. However, in the fractional encoding method, the period of MEGs is chosen to be shorter than the period of mechanical motion. The expected tradeoff would be less efficient motion encoding due to mismatched frequencies of MEG and mechanical motion, leading to lower SNR on wave images (15).

While SE-EPI-MRE sequences have been available with FDA-approved commercial implementations of MRE for several years, there is only limited information on comparability with standard one directional motion encoding GRE-MRE sequence in the literature (16). All the published data using a SE-EPI-MRE sequence in the liver used a 3 directional motion encoding SE-EPI-MRE (17–19). Moreover, there are few published data on fat and iron effects on MRE quality (20).

The objectives of our study were to compare 2D, one directional motion encoding, GRE- and SE-EPI-MRE sequences for liver MRE in terms of image quality and LS measurements and to assess the influence of liver fat and iron deposition on MRE image quality.

MATERIALS AND METHODS

Phantom study

A phantom study was performed using a previously described setup (21). Two thousand grams of 2% weight-in-weight gelatin sample was prepared by the procedure described in Clayton et al. (22) with water and 200 grams of glycerol was added to the mixture in order to reduce the water loss from the gel. The clinical MRE hardware (GE Healthcare) was used for the mechanical actuation. The passive driver was secured on top of the sample and it caused vertical motion on the container. The same MRE sequences as those used for the patients were performed.

Patients

This prospective single-center study was HIPAA compliant. Our local institutional review board approved this study and waived the requirement for informed consent. Between August 2014 and November 2014, subjects who had a liver MRI on our 3.0T GE system were enrolled. Consecutive patients with GRE and SE-EPI-MRE acquisitions were included. MRE is part of the liver MRI clinical protocol in our institution.

The final population included 50 patients (M/F 33/17, mean age 58 y, range 22–80 y). The indications of liver MRI were: chronic liver disease follow up and hepatocellular carcinoma screening/surveillance (n=44), focal liver lesions (n=4), and elevated liver enzymes (n=2). The etiologies of the chronic liver disease were: chronic viral hepatitis C (n=30), chronic viral hepatitis B (n=6), NASH (n=3), alcohol abuse (n=1), primary biliary cirrhosis (n=1), primary sclerosing cholangitis (n=1), cryptogenic cirrhosis (n=1), autoimmune hepatitis (n=1). Twenty-eight patients (28/50=56%) had cirrhosis confirmed by liver biopsy (n=4) or morphologic imaging findings (n=24) (liver surface nodularity and findings of portal hypertension).

To assess test-retest repeatability of the SE-EPI-MRE sequence, 4 additional patients (M/F 3/1, mean age 67y) had 2 SE-EPI-MRE acquisitions during the same MRI session. These cases were not used for final analysis.

MRI and MRE acquisition

Patients were not required to fast before the exam. All the exams were performed using a 3.0T system (GE Discovery MR750, GE Healthcare, Waukesha, WI) using a phased array 32 channel body coil and 50 mT/m maximum gradient strength and 200 T/m/s maximum gradient slew rate. Our liver protocol included the following sequences: axial and coronal single-shot (SS FSE) T2-weighted imaging (T2WI); axial fat-suppressed fast spin echo T2WI; axial 3D T1-weighted imaging (T1WI) in- and out-of-phase, axial diffusion weighted (DW)-imaging; axial T2* multi-echo gradient-echo sequence (TR/TE 80/1–15 ms, 16 echoes) and contrast-enhanced imaging using a 3D T1WI breath-hold fat-suppressed spoiled

GRE sequence before and after intravenous gadolinium contrast administration (gadoxetic acid, Primovist/Eovist, Bayer Healthcare).

Liver MRE sequences were performed after contrast administration (23). For MRE wave generation, a 19 cm-diameter passive acoustic driver was placed on the right side of the abdomen at the level of the xiphoid. Four axial slices were centered over the portal vein using SS FSE axial and coronal sequences. Wave imaging was performed using a modified phase contrast gradient echo sequence with motion encoding gradients along z-axis. For GRE sequence, all 4 slices were acquired in 4 consecutive breath holds at end expiration and for EPI sequence all 4 slices were acquired in a single breath hold. The details of the sequences are presented in Table 1. The timing diagrams of the 2 MRE sequences are presented in Fig. 1.

MRE image analysis

The multimodel direct inversion (MMDI) algorithm, a statistically based direct inversion algorithm, generated automatically stiffness maps from wave images (24, 25). For each MRE stiffness map, a confidence index (ranging from 0–100%) for stiffness measurement was estimated using an algorithm reflecting SNR, wave amplitude, multi-path wave interference and inversion algorithm performance and was automatically provided by the software.

Image quality analysis—Two fellowship-trained radiologists (observers 1 and 2, -- and --, with 4 and 2 years of body MRI experience) independently assessed image quality of GRE-MRE and SE-EPI-MRE acquisitions on wave propagation images and confidence maps using a 4-point scale (0–3, with 3 being the highest score) using a PACS workstation (Centricity PACS 3.2.2, GE Healthcare, Waukesha, WI). For the wave images, a single score was given for the 4 slices as follows: 0: no observable wave propagation; 1: wave propagation in approximately less than 1/3 of the liver; 2: wave propagation in approximately less than 2/3 of the liver and 3: excellent wave propagation, superior than approximately 2/3 of the liver (Fig. 2). For the confidence maps, the quality was scored for each slice: 0: no pixel with a confidence higher than 95%; 1: confidence map covering approximately less than 25% of the liver; 2: confidence map covering approximately between 25% and 50% of the liver and 3: confidence map covering approximately more than 50% of the liver (Fig. 2). An overall image quality score was computed as the sum of the wave propagation score and the confidence map score for each slice (max 15).

Quantitative analysis—MRE quantitative analysis was performed by a third observer (observer 3, --, a radiologist with 3 years of body MRI experience) using Osirix software (v 5.5.2, Geneva, Switzerland). This observer was not blinded to the nature of the sequence. Free-hand regions of interest (ROIs) were drawn on the 4 slices using 3 steps. First, the ROIs were drawn on the magnitude images to exclude large vessels, parenchyma edge and fissures; second, the ROIs were pasted on the confidence map to exclude all the pixels with a confidence index lower than 95%; and third, the ROIs were pasted on the stiffness map. LS values and ROI size were extracted. An average LS value (kPa) and an average ROI size (cm^2) were computed from all 4 slices for the 2 MRE acquisitions.

In order to compute the hepatic fat fraction (FF, %), the 3rd observer drew 2 ROIs in the right hepatic lobe on T1-weighted in-phase images. The ROIs were then pasted on the T1-weighted out-of-phase images. The fat fraction was calculated as: $FF = (SI_{IP}-SI_{OP})/2SI_{IP}$ (where SI_{IP}: signal intensity on the in-phase images, SI_{OP}: signal intensity on the out-of-phase images) (26). To estimate hepatic iron content, 2 ROIs where drawn in the right hepatic lobe on the T2* maps (27) (same location as for FF). For the phantom analysis, one ROI as large as possible was drawn on each of the 4 slices, to measure stiffness.

Statistical analysis

Results are presented as mean ± standard deviation (range) for quantitative data. Mean LS values, ROI sizes and image quality scores between SE-EPI and GRE-MRE were compared using a paired Wilcoxon test. Variability of LS between the 2 sequences was assessed with intra-class coefficient correlation (ICC), coefficient of variation (CV) and Bland-Altman limits of agreement analysis (BALA). Variability of the phantom stiffness was assessed with CV and Bland-Altman analysis. The association of fat fraction and T2* values with image quality scores, ROI size and LS was assessed by partial Spearman correlation to adjust each parameter for the other parameter. CV was used to assess test-retest repeatability for SE-EPI-MRE acquisition. All analyses were performed using Statistical Package for the Social Sciences (SPSS) software (version 20.0, IBM SPSS Inc., Armonk, New York, US) and GraphPad Prism 5.0 software (GraphPad Software, Inc., California, USA). A two-sided p value of less than 0.05 was considered statistically significant.

RESULTS

Phantom data

Phantom stiffness measurements were not significantly different between SE-EPI and GRE acquisitions, with mean stiffness of 3.24 ± 0.03 vs. 3.33 ± 0.02 kPa, respectively (p=0.068). The reproducibility of stiffness measurements between the two sequences was excellent, with mean CV of 2.8%, and Bland-Altman analysis showing very small bias of 0.09, with limits of agreement of 0.02–0.16 kPa.

Test-retest repeatability of the SE-EPI-MRE sequence

Repeatability was excellent, with mean CV of 5.4% (range 4.4% – 7.4%).

Failure rate

GRE-MRE failed in 4 patients (no pixel with a confidence index higher than 95%) while there was no case of failure with SE-EPI-MRE. 2/4 patients with GRE-MRE failure had a short T2*, indicating iron deposition (T2* = 4.4 and 11.3 ms) while the other two patients had liver cirrhosis with normal T2* values for 3.0T (T2* = 14.8 and 17.6 ms) (28, 29) and minimal steatosis (fat fraction = 7 and 9%), with large ascites in one patient (Fig. 3).

Image quality and ROI size (Table 2)

Overall image quality scores were significantly higher using SE-EPI-MRE vs. GRE-MRE for both observers (p <0.0001). For observer 1, image quality scores were higher with SE-

EPI-MRE in all patients but one. For observer 2, image quality scores were higher with SE-EPI-MRE for 47 patients, and equal for the remaining 3 patients (Fig. 4). For SE-EPI-MRE, the image quality scores were maximal (15) in 35 patients (70%) for observer 1, and 36 patients (72%) for observer 2; while for GRE-MRE maximum scores were given in 8 patients (16%) for observer 1 and only 3 patients (6%) for observer 2. ROI size was significantly larger using SE-EPI-MRE vs. GRE-MRE ($p < 0.0001$). For all patients, the ROI size was higher using SE-EPI-MRE than GRE-MRE. The mean ROI size with SE-EPI-MRE was on average 3.5 larger than that of GRE-MRE (Table 2).

Inter-sequence reproducibility of LS measurements

LS measurements were not significantly different between SE-EPI-MRE and GRE-MRE sequences ($p=0.06$) (Table 2, Fig. 5–6), with high reproducibility between the two sequences (ICC=0.909, $p < 0.0001$) (Fig. 6), and mean CV of 10.2% (range, 0.2%–28.2%). Bland-Altman analysis confirmed high reproducibility, showing minimal bias of 0.23 ± 0.73, and 95% limits of agreement of −1.19 and 1.66 kPa (Fig. 6).

Influence of liver fat and iron on image quality and LS

Twenty-eight patients had liver steatosis (defined by FF>5%) (30). There was no significant correlation between FF and image quality scores for both observers and sequences (for observer 1: GRE-MRE r 0.008, $p=0.958$, SE-EPI-MRE r −0.058, $p=0.690$; for observer 2: GRE-MRE r −0.028, $p=0.848$, SE-EPI-MRE r −0.113, $p=0.441$). In addition, there was no significant correlation between FF and ROI size for both sequences (GRE-MRE r =0.063, $p=0.669$, SE-EPI-MRE r −0.181, $p=0.214$).

Six patients had iron overload (T2* <14 ms) (28, 29). Image quality scores derived from GRE-MRE were significantly correlated with liver T2* values, while image quality scores from SE-EPI-MRE were not (observer 1: GRE-MRE r 0.607, $p < 0.0001$, SE-EPI-MRE r 0.137, $p= 0.347$; observer 2: GRE-MRE r 0.618, $p < 0.0001$, SE-EPI-MRE r 0.029, $p=0.841$) (Fig. 7). In addition, ROI size derived from GRE-MRE sequence was significantly correlated with liver T2* values (r 0.614, $p < 0.0001$) while ROI size derived from SE-EPI-MRE sequence was only weakly correlated with liver T2* (r 0.333, $p=0.020$) (Fig. 7).

There was no significant correlation between LS and T2* or LS and FF for both sequences (r −0.153 to 0.123, $p=0.317$ to 0.869).

DISCUSSION

Our results show the advantage of a SE-EPI-MRE sequence in terms of image quality and acquisition time with equivalent LS measurements compared to a standard GRE-MRE sequence. Our results are in agreement with a prior study by Huwart et al which showed higher image quality of SE-EPI-MRE sequence in the liver, compared to SE-MRE (18). However, another publication found that a GRE-based implementation outperformed an SE-EPI implementation (17). These conflicting findings indicate that the details of specific pulse sequence implementation have a significant impact on the results. The importance of the findings of this study are that SE-EPI sequences used in commercially-available MRE implementations can be expected to provide performance that is at least equivalent to that

documented in the many published studies using GRE-MRE sequences, with faster acquisition.

We also did not observe any case of failure with SE-EPI-MRE, while GRE-MRE failed in 4 cases. Better image quality with SE-EPI-MRE was expected because SE-EPI sequence is less sensitive to T2* decay than GRE sequence, and therefore less prone to iron deposition or field inhomogeneity related effects (18). The influence of iron deposition on image quality of the GRE-MRE sequence was confirmed by the strong correlation found between liver T2* values and each of image quality scores and ROI size. As expected, the T2* had a lower influence on the image quality scores using the SE-EPI-MRE sequence.

The use of a SE-EPI sequence for MRE poses some disadvantages that could potentially degrade the image quality. First, the use of EPI readout could theoretically increase the susceptibility artifacts and second the difference in frequency between the mechanical excitation and the motion-encoding gradient leads to less efficient motion encoding due to a mismatch (15). Nevertheless, this mismatch did not affect the quality of SE-EPI-MRE in our study. Another limitation of the SE-EPI sequence could be its resolution, which is lower than the one of the GRE-based acquisition. Indeed, the matrix size influences the echo train length, which, if too long, can cause distortion.

The higher quality of the SE-EPI-MRE sequence may also be explained by its shorter acquisition time, allowing the acquisition of 4 slices in a single breath-hold. The shear waves applied for MRE acquisition lead to tissue displacement that induces cyclical motion of the spins, which produces a measurable phase shift in the presence of MEGs. To obtain the wave images and the phase information, for each slice, 4 identical images are acquired with different offset between mechanical motion and the oscillating MEGs. Those 4 images need to be matched in order to obtain correct wave images. If the scan is faster, the risk of image misregistration decreases.

Moreover, degradation of image quality due to respiratory motion artifacts leading to decreased performance of abdominal MRI is a common problem in patients with diminished breath-hold capacity. This can be especially critical in patients with advanced liver disease, whose breath-hold capabilities may be diminished. Therefore, our results suggest that an SE-EPI approach could be a better alternative for LS measurement in the clinic.

In this study, SE-EPI-MRE provided larger confidence maps in comparison with GRE-MRE sequence. Increasing the coverage of the liver volume is one of the main advantages of MRE in comparison to US elastography and liver biopsy, which only allow a small sampling of liver parenchyma (31–34). The use of SE-EPI-MRE in our study allowed larger sampling of the liver parenchyma with larger ROI placement for liver stiffness evaluation, which would likely result in a more comprehensive assessment of diffuse liver disease. Moreover, because of its shorter acquisition time, it allows the acquisition of more slices and therefore increased liver coverage. Finally, equivalent LS measurements were obtained between SE-EPI and GRE-MRE sequences. Most of the published studies on MRE for liver fibrosis detection have used GRE-MRE (7, 20, 34). Therefore, before considering replacing GRE-MRE by SE-EPI-MRE, it is important to ensure that SE-EPI-MRE provides equivalent LS

measurements and accuracy for liver fibrosis detection. While the inter-sequence LS reproducibility was high, the accuracy of SE-EPI-MRE needs to be tested in a separate study.

If future studies validate the diagnostic accuracy of the SE-EPI-MRE for liver fibrosis detection, the results of this study suggest that SE-EPI-MRE sequence may be a viable alternate sequence to GRE-MRE, due to its higher quality and shorter acquisition time. The SE-EPI-MRE sequence may be especially helpful in patients with liver iron overload and patients with diminished breath-hold capabilities, in which the GRE-MRE sequence can fail (20).

Our study has several limitations. First, we did not assess SE-EPI-MRE performance for detection and staging of liver fibrosis, which was not the aim of this study. Second, although we have limited data on test-retest analysis (n=4), we observed equivalent repeatability to that reported for SE-EPI-MRE in the kidney (16), and for liver GRE-MRE (35–37).

In conclusion, SE-EPI-MRE performs superiorly than GRE-MRE in terms of image quality, liver coverage, and success rate, with shorter acquisition time while providing comparable LS values. This approach might improve the performance and clinical acceptance of liver MRE, especially in patients with iron deposition or diminished breath-hold capabilities. Future studies are necessary to assess the diagnostic performance of SE-EPI-MRE for liver fibrosis detection and staging.

Acknowledgments

Source of Funding:

This work was supported by a General Electric Healthcare grant received by the Mount Sinai Radiology Department.

Bachir Taouli is currently receiving a grant (1R01DK087877) from the NIH.

Richard Ehman is currenlty receiving a grant (EB001981) from the NIH.

Mathilde Wagner has received a grant from the Société Française de Radiologie.

Maggie Fung is an employee of GE Healthcare.

Scott A. Kruse and Roger C. Grimm

ABBREVIATIONS AND ACRONYMS

BALA	Bland-Altman limits of agreement
CV	coefficient of variation
GRE	gradient recalled echo
ICC	intraclass correlation coefficient
LS	liver stiffness
MEG	motion encoding gradient

MMDI	multimodel direct inversion
MRE	magnetic resonance elastography
ROI	region of interest
SE-EPI	spin echo echoplanar imaging
SNR	signal to noise ratio

References

1. Venkatesh SK, Ehman RL. Magnetic resonance elastography of liver. Magn Reson Imaging Clin N Am. 2014; 22(3):433–46. [PubMed: 25086938]
2. Ronot M, Lambert S, Elkrief L, et al. Assessment of portal hypertension and high-risk oesophageal varices with liver and spleen three-dimensional multifrequency MR elastography in liver cirrhosis. Eur Radiology. 2014; 24(6):1394–402.
3. Yin M, Kolipaka A, Woodrum DA, et al. Hepatic and splenic stiffness augmentation assessed with MR elastography in an in vivo porcine portal hypertension model. J Magn Reson Imaging. 2013; 38(4):809–15. [PubMed: 23418135]
4. Guo J, Buning C, Schott E, et al. In vivo abdominal magnetic resonance elastography for the assessment of portal hypertension before and after transjugular intrahepatic portosystemic shunt implantation. Invest Radiol. 2015; 50(5):347–51. [PubMed: 25599282]
5. Huwart L, Sempoux C, Salameh N, et al. Liver fibrosis: noninvasive assessment with MR elastography versus aspartate aminotransferase-to-platelet ratio index. Radiology. 2007; 245(2): 458–66. [PubMed: 17940304]
6. Shi Y, Guo Q, Xia F, et al. MR Elastography for the Assessment of Hepatic Fibrosis in Patients with Chronic Hepatitis B Infection: Does Histologic Necroinflammation Influence the Measurement of Hepatic Stiffness? Radiology. 2014; 273(1):88–98. [PubMed: 24893048]
7. Venkatesh SK, Wang G, Lim SG, et al. Magnetic resonance elastography for the detection and staging of liver fibrosis in chronic hepatitis B. Eur Radiol. 2014; 24(1):70–8. [PubMed: 23928932]
8. Dyvorne HA, Jajamovich GH, Bane O, et al. Prospective comparison of magnetic resonance imaging to transient elastography and serum markers for liver fibrosis detection. Liver Int. 2016 Jan 6. Epud ahead of print.
9. Lee Y, Lee JM, Lee JE, et al. MR elastography for noninvasive assessment of hepatic fibrosis: reproducibility of the examination and reproducibility and repeatability of the liver stiffness value measurement. J Magn Reson Imaging. 2014; 39(2):326–31. [PubMed: 23589232]
10. Runge JH, Bohte AE, Verheij J, et al. Comparison of interobserver agreement of magnetic resonance elastography with histopathological staging of liver fibrosis. Abdom Imaging. 2014; 39(2):283–90. [PubMed: 24366108]
11. Venkatesh SK, Yin M, Ehman RL. Magnetic resonance elastography of liver: technique, analysis, and clinical applications. J Magn Reson Imaging. 2013; 37(3):544–55. [PubMed: 23423795]
12. Muthupillai R, Lomas DJ, Rossman PJ, et al. Magnetic resonance elastography by direct visualization of propagating acoustic strain waves. Science. 1995; 269(5232):1854–7. [PubMed: 7569924]
13. Taouli B, Ehman RL, Reeder SB. Advanced MRI methods for assessment of chronic liver disease. AJR Am J Roentgenol. 2009; 193(1):14–27. [PubMed: 19542391]
14. Klatt D, Asbach P, Rump J, et al. In vivo determination of hepatic stiffness using steady-state free precession magnetic resonance elastography. Invest Radiol. 2006; 41(12):841–8. [PubMed: 17099421]
15. Rump J, Klatt D, Braun J, et al. Fractional encoding of harmonic motions in MR elastography. Magn Reson Med. 2007; 57(2):388–95. [PubMed: 17260354]
16. Low G, Owen NE, Joubert I, et al. Reliability of magnetic resonance elastography using multislice two-dimensional spin-echo echo-planar imaging (SE-EPI) and three-dimensional inversion

reconstruction for assessing renal stiffness. J Magn Reson Imaging. 2015; 42(3):844–50. [PubMed: 25537823]

17. Garteiser P, Sahebjavaher RS, Ter Beek LC, et al. Rapid acquisition of multifrequency, multislice and multidirectional MR elastography data with a fractionally encoded gradient echo sequence. NMR Biomed. 2013; 26(10):1326–35. [PubMed: 23712852]
18. Huwart L, Salameh N, ter Beek L, et al. MR elastography of liver fibrosis: preliminary results comparing spin-echo and echo-planar imaging. Eur Radiol. 2008; 18(11):2535–41. [PubMed: 18504591]
19. Shin SU, Lee JM, Yu MH, et al. Prediction of esophageal varices in patients with cirrhosis: usefulness of three-dimensional MR elastography with echo-planar imaging technique. Radiology. 2014; 272(1):143–53. [PubMed: 24620910]
20. Yin M, Glaser KJ, Talwalkar JA, et al. Hepatic MR Elastography: Clinical Performance in a Series of 1377 Consecutive Examinations. Radiology. 2016; 278(1):114–24. [PubMed: 26162026]
21. Yasar TK, Royston TJ, Magin RL. Wideband MR elastography for viscoelasticity model identification. Magn Reson Med. 2013; 70(2):479–89. [PubMed: 23001852]
22. Clayton EH, Okamoto RJ, Bayly PV. Mechanical properties of viscoelastic media by local frequency estimation of divergence-free wave fields. J Biomech Eng. 2013; 135(2):021025. [PubMed: 23445070]
23. Motosugi U, Ichikawa T, Sou H, et al. Effects of gadoxetic acid on liver elasticity measurement by using magnetic resonance elastography. Magn Reson Imaging. 2012; 30(1):128–32. [PubMed: 21937180]
24. Manduca A, Oliphant TE, Dresner MA, et al. Magnetic resonance elastography: non-invasive mapping of tissue elasticity. Med Image Anal. 2001; 5(4):237–54. [PubMed: 11731304]
25. Silva AM, Grimm RC, Glaser KJ, et al. Magnetic resonance elastography: evaluation of new inversion algorithm and quantitative analysis method. Abdom Imaging. 2015; 40(4):810–7. [PubMed: 25742725]
26. Fishbein MH, Gardner KG, Potter CJ, et al. Introduction of fast MR imaging in the assessment of hepatic steatosis. Magn Reson Imaging. 1997; 15(3):287–93. [PubMed: 9201675]
27. Alexopoulou E, Stripeli F, Baras P, et al. R2 relaxometry with MRI for the quantification of tissue iron overload in beta-thalassemic patients. J Magn Reson Imaging. 2006; 23(2):163–70. [PubMed: 16374880]
28. Storey P, Thompson AA, Carqueville CL, et al. R2* imaging of transfusional iron burden at 3T and comparison with 1.5T. J Magn Reson Imaging. 2007; 25(3):540–7. [PubMed: 17326089]
29. Hernando, D., Qazi, N., Reeder, S. Calibration of confounder-corrected R2* for liver iron quantification at 1.5T and 3T: preliminary results. Proceedings of the 21th Annual Meeting of ISMRM; 2013; Salt Lake City.
30. Reeder SB, Cruite I, Hamilton G, et al. Quantitative Assessment of Liver Fat with Magnetic Resonance Imaging and Spectroscopy. J Magn Reson Imaging. 2011; 34(4) spcone.
31. Bedossa P, Dargere D, Paradis V. Sampling variability of liver fibrosis in chronic hepatitis C. Hepatology. 2003; 38(6):1449–57. [PubMed: 14647056]
32. Cassinotto C, Lapuyade B, Ait-Ali A, et al. Liver fibrosis: noninvasive assessment with acoustic radiation force impulse elastography--comparison with FibroScan M and XL probes and FibroTest in patients with chronic liver disease. Radiology. 2013; 269(1):283–92. [PubMed: 23630312]
33. Castera L, Vergniol J, Foucher J, et al. Prospective comparison of transient elastography, Fibrotest, APRI, and liver biopsy for the assessment of fibrosis in chronic hepatitis C. Gastroenterology. 2005; 128(2):343–50. [PubMed: 15685546]
34. Yoon JH, Lee JM, Joo I, et al. Hepatic fibrosis: prospective comparison of MR elastography and US shear-wave elastography for evaluation. Radiology. 2014; 273(3):772–82. [PubMed: 25007047]
35. Jajamovich GH, Dyvorne H, Donnerhack C, et al. Quantitative Liver MRI Combining Phase Contrast Imaging, Elastography, and DWI: Assessment of Reproducibility and Postprandial Effect at 3.0 T. PLoS One. 2014; 9(5):e97355. [PubMed: 24840288]
36. Shi Y, Guo Q, Xia F, et al. Short- and midterm repeatability of magnetic resonance elastography in healthy volunteers at 3.0 T. Magn Reson Imaging. 2014; 32(6):665–70. [PubMed: 24650683]

37. Shire NJ, Yin M, Chen J, et al. Test-retest repeatability of MR elastography for noninvasive liver fibrosis assessment in hepatitis C. J Magn Reson Imaging. 2011; 34(4):947–55. [PubMed: 21751289]

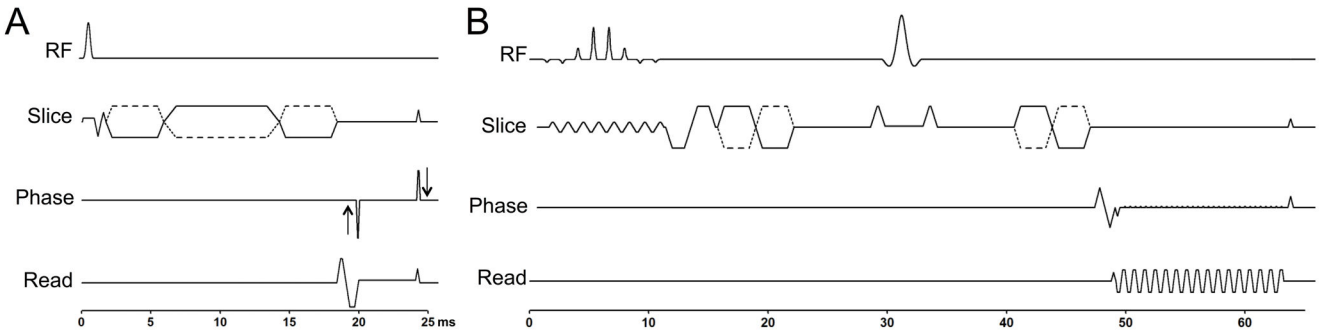

Figure 1.

Timing diagrams of the GRE (A) and the SE-EPI-MRE (B) sequences. The toggling MEG gradients are shown with dotted lines.

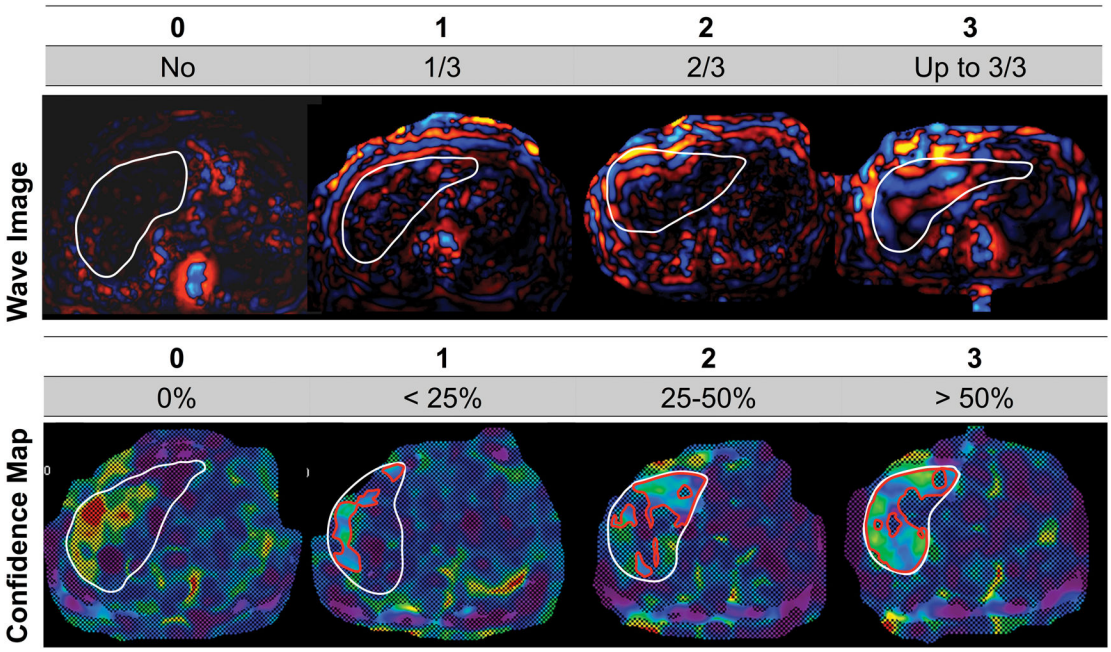

Figure 2.

Examples of GRE-MRE wave images and confidence maps illustrating the image quality scoring system. For wave images, score was based on depth of propagation of waves. For confidence maps, quality was scored for each slice, based on percentage of liver pixels with confidence higher than 95% (white line borders the liver; red contour borders the area of pixels with confidence index higher than 95%).

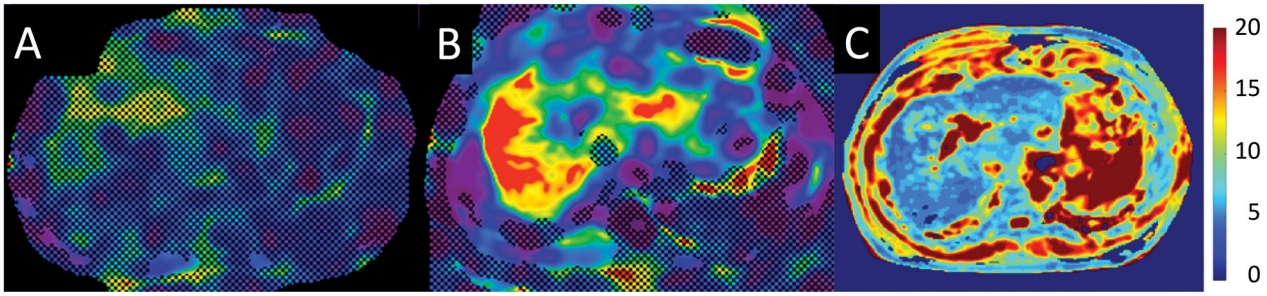

Figure 3.

Example of GRE-MRE failure in a 61-year-old male with HCV cirrhosis. The confidence map of GRE-MRE (A) showed no pixel with a confidence index higher than 95%, while most of the liver has confidence index higher than 95% with SE-EPI-MRE (B, black contour borders the analyzed ROI and white contour borders the liver). T2* map (C) showed severe iron overload with liver T2* of 4.4 ms.

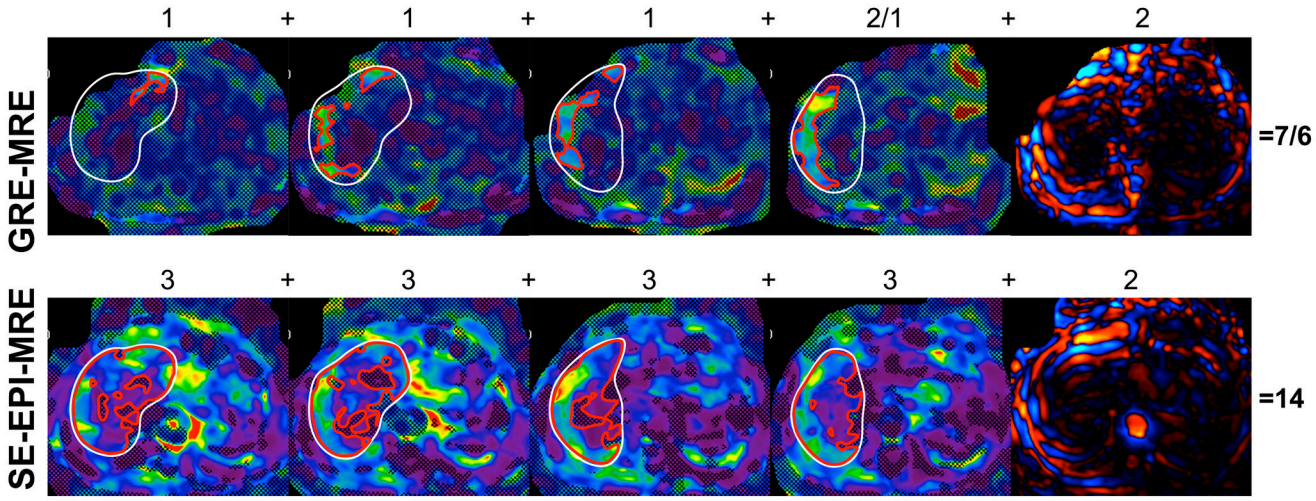

Figure 4.

Example of GRE-MRE and SE-EPI-MRE examinations in a 63-year-old male with cholangiocarcinoma without liver disease. Both observers found higher image quality scores for SE-EPI-MRE in comparison with GRE-MRE, with image quality scores of 7–6 for GRE-MRE and 14-14 for SE-EPI-MRE, respectively (white contour borders the liver, red contour borders the area of pixels with confidence index higher than 95%; the first four images represent the 4 slices of the confidence map and the fifth images represents the wave image). Numbers above the images refer to the qualitative score given by reader1/reader 2.

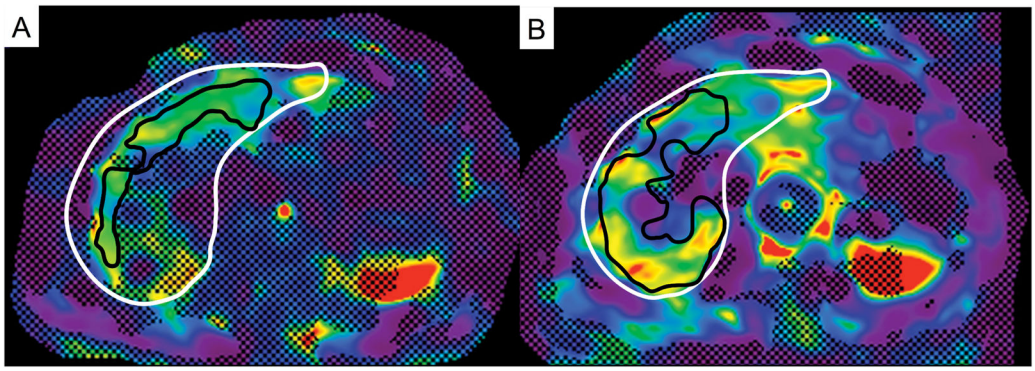

Figure 5.

Example of stiffness maps in a 69-year-old male with HCV cirrhosis. Liver stiffness (LS) was similar with the 2 sequences (GRE-MRE: 3.5 kPa, SE-EPI-MRE 3.7 kPa), with larger ROI size with SE-EPI-MRE (62 vs. 27 cm^2 with GRE-MRE). Black/white contours border the analyzed ROI/liver parenchyma.

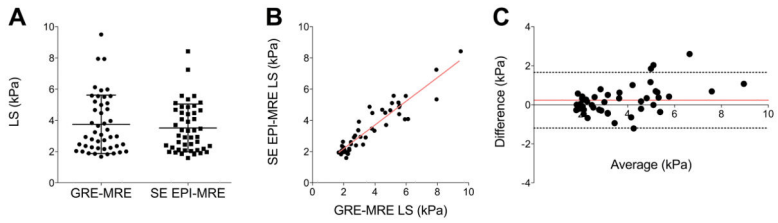

Figure 6.

Agreement and reproducibility of liver stiffness (LS) measurement obtained with GRE and SE-EPI-MRE sequences. LS was not significantly different between the 2 sequences (p=0.062) (A). There was also high reproducibility of LS with ICC=0.909 (B) and Bland-Altman limits of agreement of [−1.19; 1.66 kPa] (C).

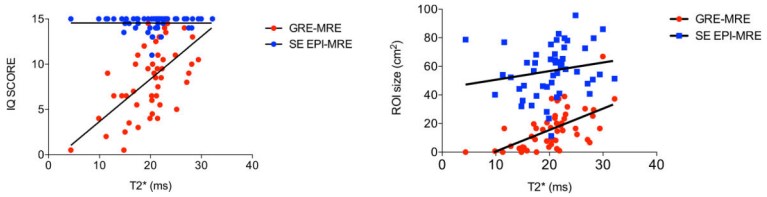

Figure 7.

Correlation between liver T2* values and image quality (IQ) scores (average of 2 observers) and between liver T2* values and ROI size. Liver T2* had an influence on GRE-MRE image quality score and on GRE-MRE ROI size as showed by the significant strong correlations (r 0.620 and r 0.614, respectively, p <0.0001).

Table 1

Sequence parameters of MRE acquisitions using GRE and EPI.

	2D GRE	2D SE-EPI
Number of slices	4	
Slice thickness	10 mm	
FOV	Similar, adapted to patient' size Range: 320–460	
Matrix	256 × 80	80 × 80
TR / TE	50 / 20	1000 / 55
Number of excitations	1	1
Number of EPI shots	NA	1
Flip angle	25°	NA
Mechanical motion frequency	60 Hz (power 50%)	
MEG	60 Hz	155 Hz
MEG amplitude	17.6 mT/m	44 mT/m
Motion encoding direction	z	z
Phase offsets	4	
ASSET	2	
Acquisition time	14s/slice (=56 s) 4 breath-holds	4s/slice (=16s) 1 breath-hold

ASSET: Array Spatial Sensitivity Encoding Technique

EPI: echoplanar imaging

FOV: field of view

GRE: gradient recalled echo

MEG: motion encoding gradient

MRE: magnetic resonance elastography

Table 2

Image quality (IQ) scores, ROI size and liver stiffness (LS) values for GRE-MRE and SE-EPI-MRE measured in 50 patients (mean ± SD and range of values are given).

	GRE-MRE	SE-EPI-MRE	p
IQ score Observer 1 *	9.2 ± 4.4 (1–15)	14.6 ± 0.7 (12–15)	< 0.0001
IQ score Observer 2 *	7.9 ± 3.9 (0–15)	14.5 ± 1.2 (8–15)	< 0.0001
ROI size (cm^2)	16.1 ± 13.7 (0–67.0)	57.0 ± 17.6 (11.3–95.7)	< 0.0001
LS (kPa) **	3.75 ± 1.87 (1.68–9.50)	3.55 ± 1.51 (1.59–8.42)	0.062

*Max IQ score is 15

**4 out of 50 patients were excluded due to complete failure of GRE-MRE.

EPI: echoplanar imaging

GRE: gradient recalled echo

IQ: image quality

LS: liver stiffness

MRE: magnetic resonance elastography